Calculation and Comparison to Experiment of Magnetoresistance in the Noble Metals*

R. V. COLEMAN, A. J. FUNES, J. S. PLASKETT, AND C. M. TAPP
Department of Physics, University of Virginia, Charlottesville, Virginia
(Received 3 September 1963)

Calculations of magnetoresistance in metals have been made taking into account the contributions of open orbits. Details of the open orbits in copper have been worked out and the specific resistance has been calculated for a number of current axes. Results of experimental measurements of transverse magnetoresistance in oriented single crystals of copper and silver are reported. These results have been compared to the calculation and both experimental and theoretical curves are given. Fermi surface neck diameters have been derived from the data and comparison is made with data obtained from magnetoacoustic attenuation experiments.

INTRODUCTION

MAGNETORESISTANCE measurements in single crystals have recently been used to give significant information on the Fermi surface in a number of metals. The interpretation of experimental curves is based on the theoretical work of Lifshitz *et al.*[1] who pointed out the possibility of open-electron orbits in many metals and the effects these will have on the magnetoresistance.

In this paper we give an extension of the work of Lifshitz and compare the details of the calculation with experimental results obtained on oriented crystals of copper and silver. In particular, a relaxation time is assumed to exist and an expression is obtained for the distribution function. Details of the open orbits in copper are worked out assuming a nearly spherical Fermi surface. Transverse magnetoresistance curves are calculated for magnetic field directions near ⟨001⟩ and currents parallel to ⟨310⟩, ⟨210⟩, ⟨110⟩, and ⟨100⟩ axes. The results are then compared to the experimental curves obtained for these same current axes.

Experimental results are also given for the Fermi surface neck diameters in copper and silver. These results are compared with recent measurements of Bohm and Easterling[2] on copper and silver using magnetoacoustic attenuation.

THE SOLUTION OF BOLTZMANN'S EQUATION

The Boltzmann equation is

$$-e(\mathbf{E}+c^{-1}\mathbf{v}\times\mathbf{H})\cdot\nabla f=-(f-f_0)/\tau$$

if a relaxation time τ is assumed to exist. The number of particles at $\mathbf{p}$ in $d\mathbf{p}$ is $2(2\pi\hbar)^{-3}f(\mathbf{p})d\mathbf{p}$ and f_0 is the unperturbed Fermi distribution regarded as a function of energy, ϵ which in its turn is a function of the momentum. With $f=f_0+\varphi$ this is

$$-e(\mathbf{E}+c^{-1}\mathbf{v}\times\mathbf{H})\cdot\nabla\varphi+\tau^{-1}\varphi=ef_0'\mathbf{v}\cdot\mathbf{E}.$$

This first-order partial differential equation for φ can easily be solved along the characteristic curves that are tangent to the force field $\mathbf{E}+\mathbf{v}\times\mathbf{H}/c$. If it is assumed that $\mathbf{E}$ is small enough then the characteristics (the orbits of the electron in momentum space) can be taken tangent to $\mathbf{v}\times\mathbf{H}$ (otherwise the current would not depend linearly on $\mathbf{E}$). Now define a parameter μ along the orbits so that if μ is changed by $d\mu$ the position on the orbit is changed by $d\mathbf{p}=\mathbf{v}\times\mathbf{n}d\mu$, where $\mathbf{H}=\mathbf{n}H$. Then

$$d\varphi/d\mu=\mathbf{v}\times\mathbf{n}\cdot\nabla\varphi$$

and the Boltzmann equation becomes

$$-\frac{1}{\alpha}\frac{d\psi}{d\mu}+\psi=\mathbf{v},$$

where

$$\varphi=e\tau f_0'\psi\cdot\mathbf{E}$$

and

$$\alpha=c/(e\tau H).$$

The solution of this equation for ψ is

$$\psi(\mu)=\alpha e^{\alpha\mu}\int_{\mu}^{\infty}e^{-\alpha\mu'}\mathbf{v}(\mu')d\mu'. \tag{1}$$

This result is given by Wilson[3] [Eq. (8.55.3)]. Note that this is the only bounded solution so in fact ψ is determined uniquely. The origin of the parameter μ is obviously irrelevant. Since

$$\alpha e^{\alpha\mu}\int_{\mu}^{\infty}e^{-\alpha\mu'}d\mu'=1,$$

ψ is a mean of $\mathbf{v}$ along the orbit by a distance of about $1/\alpha$ in the direction from which the electron has come.

* Research supported in part by the U. S. Army Research Office, Durham, and the U. S. Atomic Energy Commission.

[1] I. M. Lifshitz, M. Ia. Azbel, and M. I. Kaganov, Zh. Eksperim. i Teor. Fiz. **31**, 63 (1956) [translation: Soviet Phys.—JETP **4**, 41 (1957)].

[2] Henry V. Bohm and Vernon J. Easterling, Phys. Rev. **128**, 1021 (1962).

[3] A. H. Wilson, *The Theory of Metals* (Cambridge University Press, New York, 1953).

The conductivity tensor is easily shown to be

$$\sigma=\frac{2}{(2\pi\hbar)^3}e^2\tau\int \mathbf{v}\psi\frac{dS}{v}$$

integrated over the Fermi surface inside the Brillouin zone. This surface integral can be written as a double integral by using the parameters μ and $p_{\parallel}$ (the component of the momentum parallel to **H**); the result is

$$\sigma=\frac{2}{(2\pi\hbar)^3}e^2\tau\int\int \mathbf{v}\psi d\mu dp_{\parallel}. \tag{2}$$

If α is large we have the formula

$$\psi=\mathbf{v}+\mathbf{v}'/\alpha+O(1/\alpha^2)$$

obtained by integrating by parts the integral for ψ. This gives the usual expansion of the conductivity for small τH (high temperatures and low fields), e.g., the first term gives the conductivity tensor at zero field [cf., Wilson Eq. (8.2.6)].[3]

If α is small ψ will depend on a long stretch of the orbit and this will mean that the conductivity will, in general, be a very complicated function of the direction of the magnetic field. But if the orbit is periodic (i.e., either closed or open and periodic) then the integral for ψ need only be performed over one period and

$$\psi(\mu)=\frac{\alpha e^{\alpha\mu}}{1-e^{-\alpha\mu_0}}\int_0^{\mu_0} e^{-\alpha\mu'}\mathbf{v}(\mu')d\mu'-\alpha e^{\alpha\mu}\int_0^{\mu} e^{-\alpha\mu'}\mathbf{v}(\mu')d\mu',$$

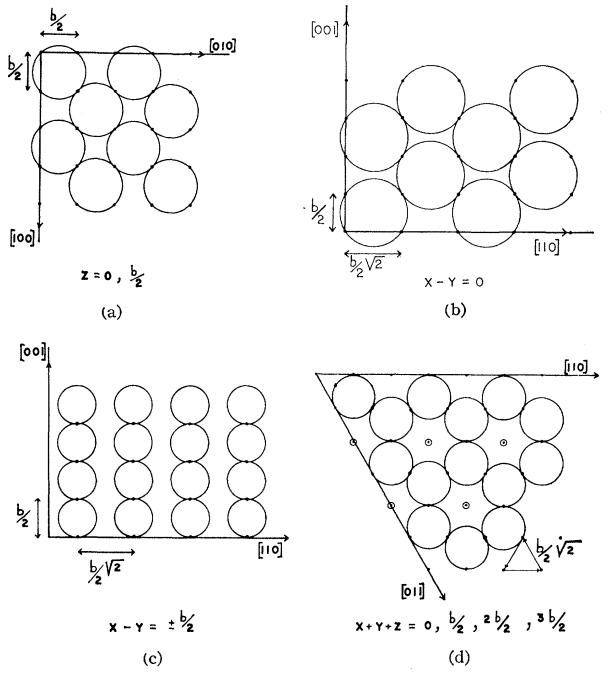

FIG. 1. Planes containing a two-dimensional lattice of necks connected together by the spherical part of the Fermi surface. (a) Section parallel to (001) for $z=0$, $(b/2)$; (b) section parallel to $(1\bar{1}0)$ for $x-y=0$; (c) section parallel to $(1\bar{1}0)$ for $x-y=\pm(b/2)$; (d) section parallel to $(\bar{1}11)$ for $x+y+z=0$, $(b/2)$, $(2b/2)$, $(3b/2)$.

where μ_0 is the period. The second term is a particular integral and the first term a solution of the homogeneous equation for ψ.

If $\alpha\mu_0$ is small this can be expanded in ascending powers of α the first term of which is

$$\psi=\frac{1}{\mu_0}\int_0^{\mu_0}\mathbf{v}(\mu')d\mu'+\cdots$$

as would be expected from the fact that ψ is a weighted mean of **v**. The projection of ψ perpendicular to **H** can easily be calculated from

$$d\mathbf{p}/d\mu=\mathbf{v}\times\mathbf{n}$$

or

$$\mathbf{v}_{\perp}=\mathbf{n}\times d\mathbf{p}/d\mu,$$

so

$$\psi_{\perp}=\mu_0^{-1}\mathbf{n}\times\Delta\mathbf{p}+\cdots, \tag{3}$$

where $\Delta\mathbf{p}$ is the difference of momentum from beginning to end of the period. If the orbit is closed this first term in the series is zero and the next term reduces to

$$\psi_{\perp}(\mu)=\alpha\left\{-\frac{1}{\mu_0}\int_0^{\mu_0}\mu'\mathbf{v}_{\perp}(\mu')d\mu' -\mathbf{n}\times[\mathbf{p}(\mu)-\mathbf{p}(0)]\right\}+\cdots. \tag{4}$$

Equations (3) and (4) were obtained by Lifshitz *et al.*[1] [Eqs. (20), (21), and (19), respectively], but of course the value of the constant part of (4) and the magnitude of the vector in (3) are not given by them since these depend on the existence of a relaxation time. Note that for a closed orbit μ_0 is the rate of change of the area of the orbit with energy and Lifshitz *et al.*[1] defined the effective mass for the orbit by

$$\mu_0=2\pi m^*.$$

DESCRIPTION OF THE FERMI SURFACE OF Cu AND Ag

The reciprocal lattice is body-centered cubic and if the cube is of side b then $\frac{1}{2}b(\pm1,\pm1,\pm1)$ are basis vectors for this lattice. The volume of the Brillouin zone is $b^3/2$ and a sphere of half this volume has the radius 0.391 b. The Fermi surface consists of a set of such spheres centered at each lattice point, except that the spheres are slightly deformed and, in fact, join together through necks in the $\langle111\rangle$ directions where the undeformed spheres are only 0.084 b apart. The centers of these necks (the center of the hexagonal faces of the zone) are at the points $\frac{1}{4}b(\pm1,\pm1,\pm1)$ plus any reciprocal lattice vector. If the origin is moved to $-\frac{1}{4}b(1,1,1)$ then it is easily shown that the centers of all the necks are at the points $\frac{1}{2}b(l,m,n)$, where l, m, and n are arbitrary integers, i.e., the necks are on a simple cubic lattice where the cube has side $b/2$. The origin has been chosen at a neck and there is a sphere centered at $\frac{1}{4}b(1,1,1)$.

There are several planes that contain a two-dimensional lattice of necks that are all connected together by the spherical part of the Fermi surface. These are the planes $z=0$, $b/2$, $x-y=0$ (but not $\pm b/2$), and $x+y+z=0$, $(b/2)$, $2(b/2)$, $3(b/2)$, and the section of the Fermi surface by these planes is shown in Fig. 1. The orbits in these planes are all closed.

It is clear that if the orbit plane is tilted through a small angle θ about some axis in one of these planes (except $x-y=\pm b/2$), say about an axis in the direction $[lm0]$ in the plane $z=0$, then the tilted plane will not cut through the necks some distance from the axis and there will be an open orbit with a mean direction $[lm0]$. In fact, if the necks extend a height h above and below $z=0$, i.e., the planes $z=\pm h$ just traverse the necks, then necks will only be traversed within a distance $h\cot\theta$ of the axis (for small h) until the tilted plane intersects the planes of necks $z=\pm b/2$. If, however, the tilt of the orbit plane is too large it will be impossible to traverse necks indefinitely in the $[lm0]$ direction and the orbit will be closed, unless the axis $[lm0]$ contains a line of connected necks. The axes [100], [110], and [010] contain such lines of connected necks and no matter how large the tilt of the orbit plane there are always open orbits for these axes. The axes [110], [111], and [001] in the $(1\bar{1}0)$ plane and the axes $[01\bar{1}]$, etc., in the (111) plane are similar lines of necks.

Now consider the axis [310]. For brevity, use $b/2$ as a unit of length so that the plane $z=0$ has a square lattice of necks and the side of the square is 1. Take the magnetic field in the direction $[1\bar{3}\lambda]$ so that the orbit planes are

$$x-3y+\lambda z=p \tag{5}$$

and these planes are tilted by θ from the plane $z=0$, where $\tan\theta=10^{1/2}\lambda$. If the necks extend a distance h above and below the plane $z=0$ (as above) then in order that the plane, Eq. (5), should go through the neck at $(x,y,0)$ (x, y integers) it is necessary that

$$x-3y-\lambda h<p<x-3y+\lambda h.$$

From this it is easy to find the possible types of orbit for each value of λh. At the critical values of λh: 1, $\frac{3}{2}$, 2, $\frac{5}{2}$, 3, $\cdots$ a new line of necks can be traversed and the type of open-orbit changes. For $\lambda h<1$ there are no open orbits. In Fig. 2, the section of the Fermi surface by the above plane is shown for λh up to 3. It will be noticed that there are two types of open orbits, one has a period of 6 quarter-circles and is seen in $1<\lambda h<\frac{3}{2}$, the other has a period of 10 quarter-circles and can be

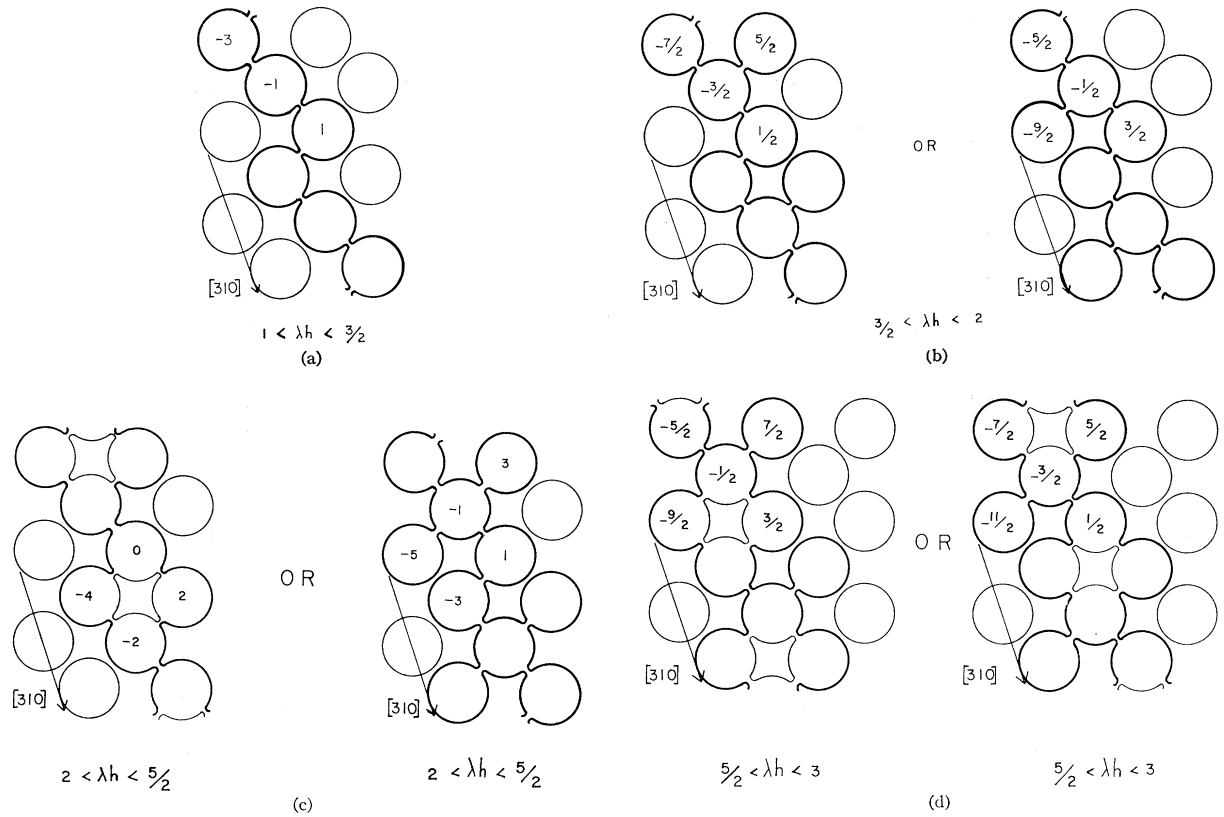

FIG. 2. Open orbits for the [310] direction. (a) Simple open orbit for $1<\lambda h<\frac{3}{2}$, period of 6 quarter-circles; (b) 10 quarter-circle period open orbit for $\frac{3}{2}<\lambda h<2$; (c) 6 or 10 quarter-circle period open orbit for $2<\lambda h<\frac{5}{2}$; (d) 6 or 10 quarter-circle period open orbit for $\frac{5}{2}<\lambda h<3$.

seen in $\frac{3}{2}<\lambda h<2$. These open orbits have the smallest value of μ_0 apart from those for the [100] and [110].

The next shortest period for an open orbit is 12 quarter-circles and occurs for the axis [210]. If the magnetic field is in the direction $[1\bar{2}\lambda]$ and the orbit plane is

$$x-2y+\lambda z=p,$$

where the angle of tilt is now given by $\tan\theta=5^{1/2}/\lambda$. Again the critical values of λh are 1, $\frac{3}{2}$, 2, $\frac{5}{2}$, $\cdots$ and there are no open orbits for $\lambda h<1$. The open orbits are all the same and those that occur up to $\lambda h=2$ are shown in Fig. 3.

The periods for open orbits in all other directions are much larger except for the [100] and [110] directions. For [100] the period is just 4 quarter-circles and for [110] the period is 2 or 6 quarter-circles. For the [100] axis take the magnetic field in the direction $[01\lambda]$ and the plane of the orbit

$$y+\lambda z=p.$$

At $\lambda h=\frac{1}{2}$, 1, $\frac{3}{2}$, 2, $\cdots$ new rows of necks are added and the open orbits up to $\lambda h=\frac{3}{2}$ are shown in Fig. 4.

For the [110] axis take the magnetic field in the direction $[1\bar{1}\lambda]$ and the plane of the orbit to be

$$x-y+\lambda z=p.$$

Again $\lambda h=\frac{1}{2}$, 1, $\frac{3}{2}$, $\cdots$ are critical and orbits for λh up to $\frac{3}{2}$ are shown in Fig. 5.

It is easily seen from Fig. 1 that for **H** near $[1\bar{1}0]$ the axes [331], [113], [221], [112], [110], [001], and [111] have similar open orbits to those that we have described for the [310], [210], [100], and [110] axes for **H** near [001].

CALCULATION OF THE MAGNETORESISTANCE

Free-Electron Fermi Surface

Since the necks are quite small most of the orbits are just circles (approximately) and the first step to understanding the resistance is to calculate the contribution to the conductivity tensor from circular

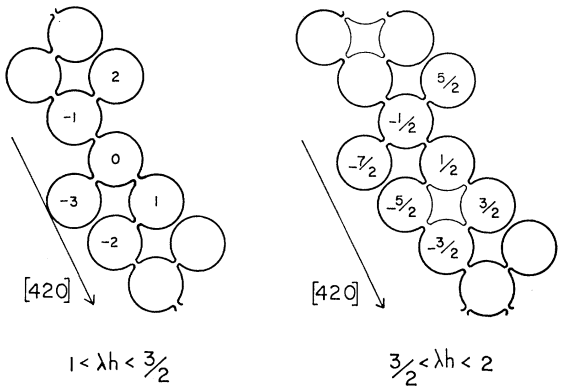

FIG. 3. Open orbits occurring for the [210] direction up to $\lambda h=2$.

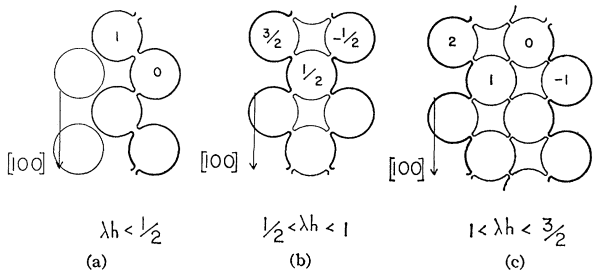

FIG. 4. Open orbits occurring for the [100] direction up to $\lambda h=\frac{3}{2}$.

orbits. We shall just assume $\epsilon=p^2/2m$ so that $d\mu=md\theta$ on the circle. At the point on the circle for which $\psi_\perp$ is required we suppose $\theta=0$ and use rectangular axes as shown in Fig. 6.[3a]

Then $\psi_{11}=v_{11}$ and

$$\psi_\perp=\alpha\int_0^\infty e^{-\alpha m\theta}v_\perp(\cos\theta,\sin\theta)md\theta$$

$$=v_\perp\cos\beta(\cos\beta,\sin\beta),$$

where $0<\beta<\pi/2$ and $\cot\beta=\alpha m$, i.e., $\psi_\perp$ has the magnitude $v_\perp\cos\beta$ and is rotated by β from $\mathbf{v}_\perp$. All appearances to the contrary this is the same as Wilson's[3] Eq. (8.51.3). The $\perp$ components of the conductivity tensor are determined by

$$\int\mathbf{v}_\perp\psi_\perp d\mu=mv_\perp^2\cos\beta\int_0^{2\pi}(\cos\theta,\sin\theta)\times(\cos(\theta+\beta),\sin(\theta+\beta))d\theta$$

$$=\pi mv_\perp^2\cos\beta\begin{bmatrix}\cos\beta\sin\beta\\-\sin\beta\cos\beta\end{bmatrix}.$$

Also

$$\int v_{11}\psi_{11}d\mu=2\pi mv_{11}^2\quad\text{and}\quad\int\mathbf{v}_\perp\psi_{11}d\mu=\int v_{11}\psi_\perp d\mu=0.$$

If all the orbits were circular and the Fermi surface was a sphere the conductivity tensor would be obtained by just integrating the above results with respect to p_{11} which gives

$$\boldsymbol{\sigma}=\frac{1}{3\pi^2}\frac{e^2\tau p^3}{\hbar^3 m}\begin{bmatrix}\cos^2\beta & \cos\beta\sin\beta & 0\\ -\cos\beta\sin\beta & \cos^2\beta & 0\\ 0 & 0 & 1\end{bmatrix},\qquad(6)$$

which is just the sum of a projection operator parallel to **H** and a rotation operator through the angle $(-\beta)$ about **H** (together with a scale factor).

[3a] *Note added in proof.* A left-handed coordinate system has been used in Fig. 6. The final answer is not affected, but a right-handed system can be constructed by placing $\psi_\perp$ and $\mathbf{V}_\perp$ in the fourth quadrant and measuring θ in a clockwise direction. The minus sign in the conductivity tensor (Eq. 6) is then shifted to the other $\cos\beta\sin\beta$ term.

The resistivity tensor is the reciprocal of this:

$$\varrho=3\pi^2\frac{\hbar^3 m}{e^2\tau p^3}\begin{pmatrix}1 & -\tan\beta & 0\\ \tan\beta & 1 & 0\\ 0 & 0 & 1\end{pmatrix}$$

and it is clear that if the potential drop is measured in the direction of the current the result is just the same as if $\beta=0$, i.e., there is no magnetoresistance. However, the electric field is rotated by β away from the current so that there is a Hall effect and β is the Hall angle.

Open Orbits

We first consider in detail the calculation of the magnetoresistance when the current is parallel to [310] and the magnetic field is near the [001] direction. In Fig. 2 the possible open orbits are shown when the magnetic field is tilted by θ from [001] and θ is decreased (as λ is increased) from the value at which open orbits appear for the first time ($\tan\theta=10^{1/2}h$) to the value at which closed hole orbits appear for the first time ($\tan\theta=10^{1/2}h/2$). Consider first the region of λ, $1<\lambda h<\frac{3}{2}$, and suppose the central Brillouin zone has its necks at the points $(x,y)=(0,0)$, $(1,0)$, $(0,1)$, and $(1,1)$ on the planes $z=0$ and $z=1$. Then, if p in Eq. (5) lies between the values $-3\pm(\lambda h-1)$, the necks at $(0,1)$, $(1,1)$, and $(2,2)$ are traversed and in Fig. 2(a) the circle with -3 inside it is the section of the Fermi surface inside the central zone. If p lies in $-1\pm(\lambda h-1)$ the necks at (0,0) (1,1) (2,1) are traversed and the circle with -1 inside it is inside the central zone. Finally, if p lies in $1\pm(\lambda h-1)$, the necks at (0,0) (1,0) (2,0) are traversed and the $+1$ circle is in the central zone. There are, therefore, three separate ranges of momentum parallel to H for which there is an open-orbit traversing the central zone near $z=0$ and each of these ranges is of thickness $2(\lambda h-1)/(10+\lambda^2)^{1/2}$.

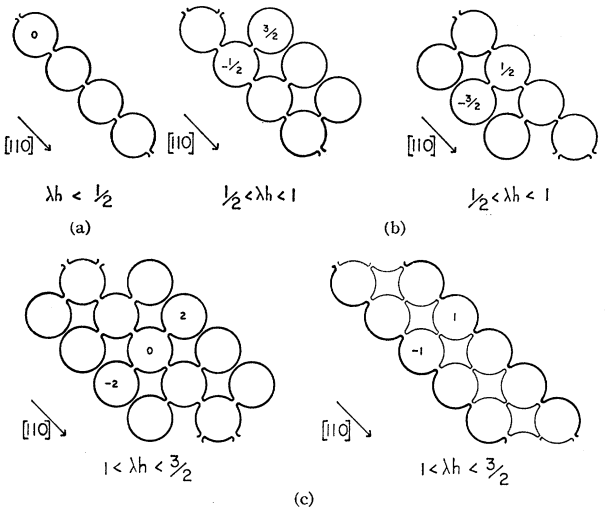

FIG. 5. Open orbits occurring for the [110] direction up to $\lambda h=\frac{3}{2}$.

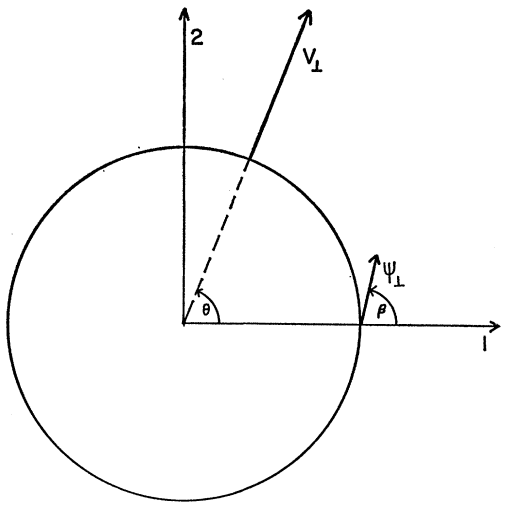

FIG. 6. Plot showing relative directions of $\mathbf{v}_\perp$ and $\psi_\perp$.

If τH is large then ψ is a constant all along one of these orbits and we can calculate $\psi_\perp$ from Eq. (3), where $\Delta\mathbf{p}=(3,1,0)$ and

$$\psi_\perp=(3\pi m)^{-1}\mathbf{n}\times(3,1,0),$$

since the length of a quarter-circle of orbit in units of μ is $m\pi/2$. Now consider the interval of p, $-3\pm(\lambda h-1)$, then (integrating only inside the central zone)

$$\int\mathbf{v}_\perp\psi_\perp d\mu=2\mathbf{n}\times(1,0,0)(3\pi m)^{-1}\mathbf{n}\times(3,1,0)$$

(the 2 is due to the fact that there are two open orbits). The integral over this range of p_{11} multiplies the above result by $2(\lambda h-1)/(10+\lambda^2)^{1/2}$. Note that this must be multiplied by $(b/2)^3$ if the dimensionless unit of momentum is not used. The calculation for the other two ranges of p is the same and, if the three answers are added and multiplied by 2 to account for the similar orbits near the plane $z=1$, we find

$$\sigma_{\perp\perp}=\frac{2e^2\tau}{(2\pi\hbar)^3}\left(\frac{b}{2}\right)^3\frac{1}{\pi m}\mathbf{n}\times(3,1,0)\mathbf{n}\times(3,1,0)\tfrac{1}{10}\xi, \quad (7)$$

where

$$\xi(\lambda)=10-\frac{4}{3}\frac{2(\lambda h-1)}{(10+\lambda^2)^{1/2}}, \quad (8)$$

for the contribution to the conductivity tensor due to open orbits if $1<\lambda h<\frac{3}{2}$.

For $\frac{3}{2}<\lambda h<2$ the open orbits just considered are still possible, for example with p in the range $-3\pm(2-\lambda h)$, and the contribution to the conductivity tensor due to them is given by Eq. (7) with

$$\xi(\lambda)=10-\frac{4}{3}\frac{2(2-\lambda h)}{(10+\lambda^2)^{1/2}}$$

and these orbits are of diminishing importance. There are also new orbits as shown in Fig. 2(b); e.g., if p is in the range $-\frac{7}{2}\pm(\lambda h-\frac{3}{2})$ then the necks at (0,1), (1,1), (2,2), and (1,2) are traversed, if (2,1) is traversed instead of (1,2) then p has to be in the range $-\frac{5}{2}\pm(\lambda h-\frac{3}{2})$. The thickness of these ranges of p_{11} is

$$2(\lambda h-\tfrac{3}{2})/(10+\lambda^2)^{1/2}.$$

For the contorted orbits on the right that occur when p is near $-\frac{7}{2}$, $-\frac{3}{2}$, $\frac{1}{2}$, and $\frac{5}{2}$, $\psi_\perp$ is

$$(5\pi m)^{-1}\mathbf{n}\times(3,1,0),$$

and the contribution of these to $\sigma_{\perp\perp}$ is given by Eq. (7) with

$$\xi(\lambda)=10\,\frac{1}{5}\,\frac{2(\lambda h-\frac{3}{2})}{(10+\lambda^2)^{1/2}}.$$

For the simple orbits on the right that occur when p is near $-\frac{5}{2}$, $-\frac{1}{2}$, $\frac{3}{2}$

$$\xi(\lambda)=10\,\frac{1}{3}\,\frac{2(\lambda h-\frac{3}{2})}{(10+\lambda^2)^{1/2}}.$$

Similarly, with the orbits on the left and orbits near $z=1$. The result for $\sigma_{\perp\perp}$ is Eq. (7) with

$$\xi(\lambda)=10\,\frac{4}{3}\,\frac{2(2-\lambda h)}{(10+\lambda^2)^{1/2}}+10\left(\frac{4}{5}+\frac{4}{3}\right)\frac{2(\lambda h-\frac{3}{2})}{(10+\lambda^2)^{1/2}}. \quad (9)$$

For $2<\lambda h<\frac{5}{2}$ the open orbits shown in Fig. 2(b) are still possible though their thickness is now decreasing and the orbits shown in Fig. 2(c) begin to appear near $p=-4$, -2, 0, 2 and $p=-5$, -3, -1, 1, 3. For this range of λh $\sigma_{\perp\perp}$ is given by Eq. (7) with

$$\xi(\lambda)=10\left(\frac{4}{5}+\frac{4}{3}\right)\frac{2(\frac{5}{2}-\lambda h)}{(10+\lambda^2)^{1/2}}+10\left(\frac{4}{5}+\frac{4}{3}\right)\frac{2(\lambda h-2)}{(10+\lambda^2)^{1/2}}$$
$$=10(32/15)(10+\lambda^2)^{-1/2}. \quad (10)$$

A little thought will show that this result remains true for all $\lambda h>2$.

The above calculation only gives four of the nine components of the conductivity tensor and those only for the open orbits. In fact this is enough to estimate the magnetoresistance as we shall now show. First let us choose new rectangular axes 1, 2, and 3 that are parallel to (3,1,0), $\mathbf{n}\times(3,1,0)$, and $\mathbf{n}$, respectively. The $\sigma_{\perp\perp}$ that we have just calculated in this system of coordinates (σ_{ij}, $ij=1, 2$) can be written

$$\frac{1}{3\pi^2}\frac{e^2\tau p^3}{\hbar^3 m}\begin{bmatrix}0 & 0\\ 0 & A\xi\end{bmatrix}, \quad (11)$$

where

$$A=\frac{3}{4\pi^2}\left(\frac{b}{2p}\right)^3=1/(2\pi)=0.159,$$

and the factor in front of the expression has been chosen to be the same as for the free-electron conductivity Eq. (6). We must add to Eq. (11) the result for all the circular orbits which will nearly be Eq. (6) if the necks are small. Now if we use the fact that α is small then β is near $\pi/2$ and $\sin\beta=1+\cdots$, $\cos\beta=\alpha m+\cdots$, and again assuming the necks are small the 1, 1 component of the resistivity tensor, i.e., the specific resistance in the [310] direction, is

$$3\pi^2\frac{\hbar^3 m}{e^2\tau p^3}\left(\frac{A\xi}{\alpha^2 m^2}\right)+\cdots. \quad (12)$$

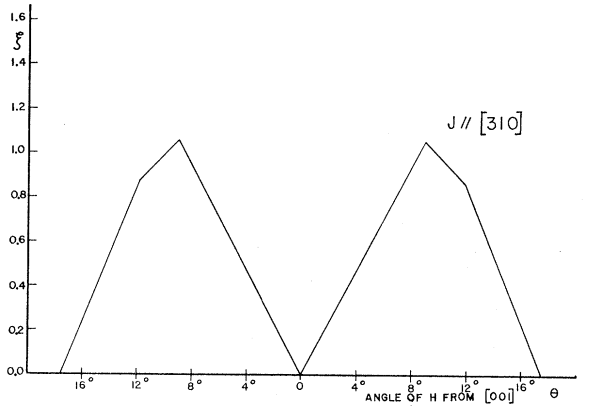

FIG. 7. Graph showing calculated values of the function $\xi(\lambda)$ as the magnetic field sweeps through the [001] pole. Current parallel to [310]. Specific resistance is a constant times this function.

The function $\xi(\lambda)$ from Eqs. (8), (9), and (10) is shown in Fig. 7 with h taken to be 0.1, which is close to the experimental value found for copper. It will be noticed that the break in the curve at $\theta=11.9°$ is due to the two types of open orbit, in effect the contorted orbit pulls down the maximum of ξ.

For the [210] current direction the open orbits for $\mathbf{H}$ near [001] are all of the same type (Fig. 3) and it is easily shown that

$$\sigma_{\perp\perp}=\frac{2e^2\tau}{(2\pi\hbar)^3}\left(\frac{b}{2}\right)^3\frac{1}{\pi m}\mathbf{n}\times(4,2,0)\mathbf{n}\times(4,2,0)\frac{1}{20}\xi,$$

where

$$\xi(\lambda)=20\times\frac{4}{6}\,\frac{2(\lambda h-1)}{(5+\lambda^2)^{1/2}}, \qquad 1<\lambda h<\tfrac{3}{2}$$
$$=20(4/6)(5+\lambda^2)^{-1/2}, \quad \tfrac{3}{2}<\lambda h. \quad (13)$$

The function ξ is shown in Fig. 8 with h again taken to be 0.1. The resistance is given by Eq. (12) with this new ξ, but the same A.

For the [100] current direction the open orbits are again all of the same type (Fig. 4) and

$$\sigma_{\perp\perp}=\frac{2e^2\tau}{(2\pi\hbar)^3}\left(\frac{b}{2}\right)^3\frac{1}{\pi m}\mathbf{n}\times(2,0,0)\mathbf{n}\times(2,0,0)\tfrac{1}{4}\xi,$$

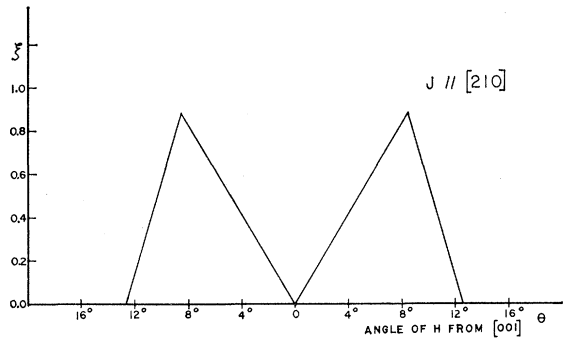

FIG. 8. Calculated values of $\xi(\lambda)$ plotted for the [001] pole and [210] current direction.

where

$$\xi(\lambda)=4\times\frac{4}{2}\frac{2\lambda h}{(1+\lambda^2)^{1/2}}, \quad \lambda h<\tfrac{1}{2}$$
$$=4(4/2)(1+\lambda^2)^{-1/2}, \quad \lambda h>\tfrac{1}{2}. \tag{14}$$

The resistance is again given by Eq. (12) and ξ is shown in Fig. 9.

For the [110] current direction the open orbits are of two types (Fig. 5) with $\mu_0=\pi m$ or $3\pi m$ and

$$\sigma_{\perp\perp}=\frac{2e^2\tau}{(2\pi\hbar)^3}\left(\frac{b}{2}\right)^3\frac{1}{\pi m}\mathbf{n}\times(110)\mathbf{n}\times(110)\tfrac{1}{2}\xi,$$

where

$$\xi(\lambda)=2\times\frac{4}{1}\frac{2\lambda h}{(2+\lambda^2)^{1/2}}, \quad \lambda h<\tfrac{1}{2}$$
$$=2\times\frac{4}{1}\frac{2(1-\lambda h)}{(2+\lambda^2)^{1/2}}+2\left(\frac{4}{3}+\frac{4}{1}\right)\frac{2(\lambda h-\frac{1}{2})}{(2+\lambda^2)^{1/2}}, \quad \tfrac{1}{2}<\lambda h<1$$
$$=2(16/3)(2+\lambda^2)^{-1/2}, \quad \lambda h>1. \tag{15}$$

The resistance is given by Eq. (12) and ξ is shown in Fig. 10. The break in the curve at $\theta=8°$ is due to the two types of open orbits.

For **H** near $[1\bar{1}0]$ and the current directions [331] and [113] there will be a resistance similar to that found for the [310] axis above, i.e., with a break in it due to two types of open orbits. For the [221] and [112] current directions the resistance is similar to that found for the [210] axis above and there will be no break because there is only one type of open orbit. For currents in the directions [110] and [001] the resistance is like the [100] case above and has no break, but the [111] axis has a break, since it is like the [110] case above.

EXPERIMENTAL RESULTS

Transverse magnetoresistance measurements have been made on a large number of oriented specimens of copper and silver and the results analyzed according to the theory discussed above. In the case of copper, specimens 15 to 20 mm long with 1-mm² cross sections were prepared by acid sawing from large copper single crystals. Back reflection Laue techniques were used to orient the crystal for cutting. Final accuracy of the sample axis orientation was $\frac{1}{2}°$. The specimens were mounted in a sample holder and immersed in a bath of liquid helium. Ratios of the room temperature resistance to the resistance at 4.2°K ranged from 1500 to 1800 for the as grown samples. In a number of cases the ratio was increased to 4000–5000 by oxidizing the sample for 24 h before making measurements. This increased the magnetoresistance anisotropy by a factor of 5, but data taken before and after oxidation gave the same result for the angles between maxima.

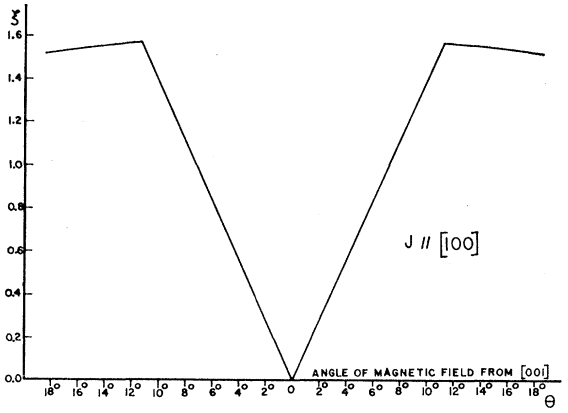

FIG. 9. Calculated values of $\xi(\lambda)$ plotted for the [001] pole and [100] current direction.

The silver specimens were prepared by growing randomly oriented single crystals six inches long with a square cross section 1 mm on a side. Seventy crystals have been grown and fifteen were selected whose axes were within one degree of the stereo triangle boundary. Specimens $2\frac{1}{2}$ in. long were cut from these crystals. Both 99.999% and 99.9999% purity silver was used.

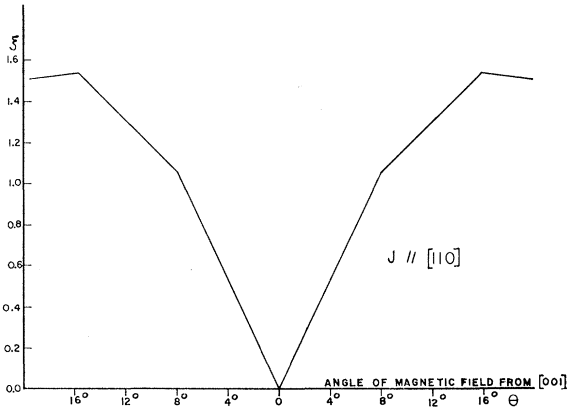

FIG 10. Calculated values of $\xi(\lambda)$ plotted for the [001] pole and [110] current direction.

The resulting room temperature to helium temperature resistance ratio was 500 and 1000, respectively.

All of the measurements have been made in a magnetic field of 13 500 G. The potential drop across the specimen was measured with a Rubicon microvolt potentiometer, the unbalance of which was fed into a photoelectric galvanometer and amplifier system driving a chart recorder. The sensitivity of the system was 5×10^{-9} V. A recorder tracing of the potential drop across the sample was made as the magnet was rotated through 360° with the field perpendicular to the sample axis.

Experimental rotation diagrams are shown for copper and silver in Fig. 11. The high double peaks occurring symmetrically about the low-index poles are due to the open-orbit regions discussed above in the theoretical section. These maxima in the resistance show an H^2 field dependence and the angle of separation can be used to calculate the neck diameter of the Fermi surface.

The maxima are located inside the open-orbit regions and as was pointed out in the section on calculation of magnetoresistance, the maxima occur at an angle for which closed hole orbits are first possible. This can be seen for example in Fig. 2(c) for the [310] current axis. The closed hole orbit is indicated by the light closed curves and first occurs for $\lambda h=2$. The function ξ has its maximum value at the corresponding value of θ which is considerably less than the value of θ for which open orbits first occur, i.e., $\tan\theta=10^{1/2}\,h$ or $\lambda h=1$. The angle between the two maxima for each current direction can be used to give an independent determination of the

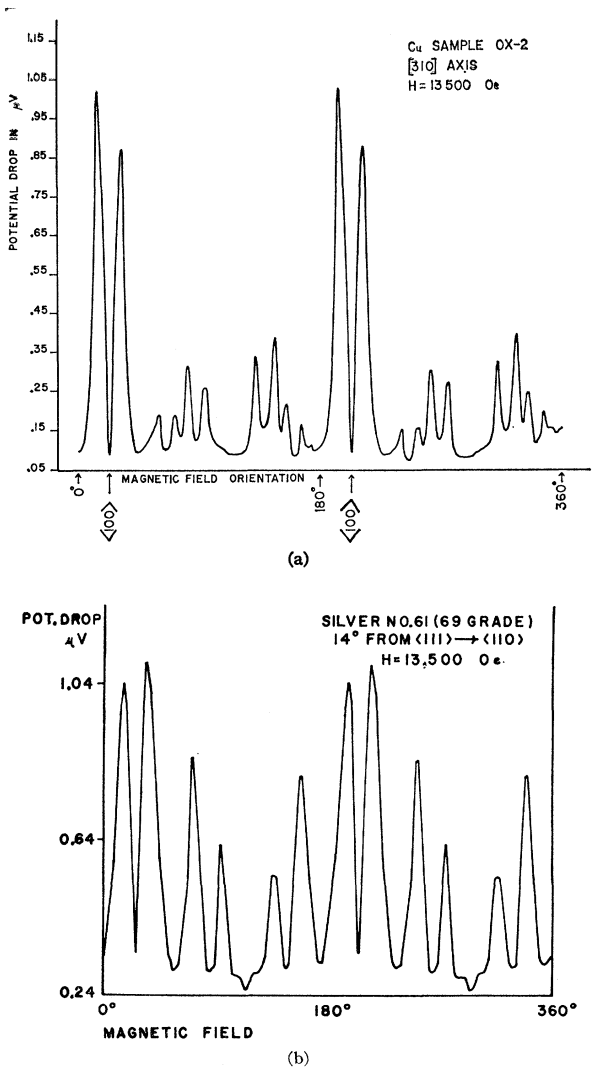

FIG. 11. Transverse magnetoresistance rotation curves obtained for copper and silver. (a) Recorder trace for [310] axis of copper; (b) recorder trace for silver. Crystal axis 14° off ⟨111⟩ toward ⟨110⟩.

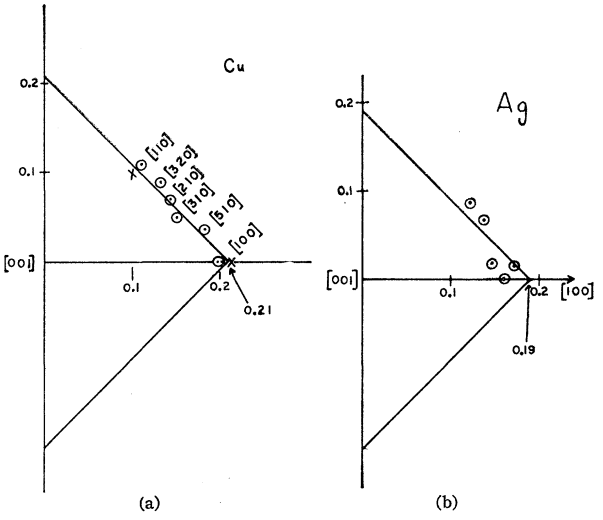

FIG. 12. Gnomonic projection of data obtained for the [001] pole. Polar coordinates are used with ϕ as the angle and $\tan\theta$ as the radius. ϕ is the angle between the current direction and the direction $[1\bar{1}0]$. θ=angle at which hole orbits first occur. The half-squares are drawn using the formula $\tan\theta\sin\phi=2h_{[001]}/\sqrt{2}$. (a) Data from copper. (b) Data from silver.

Fermi surface neck height h. For field directions sweeping through the [001] pole it is readily verified that if ϕ is the angle between the current direction and the direction $[1\bar{1}0]$, then hole orbits first occur at an angle θ given by

$$\tan\theta\sin\phi=2h_{[001]}/\sqrt{2}\,,\quad \frac{\pi}{4}<\phi<\frac{3\pi}{4}\,,$$

where h is in units of $(b/2)$.

If polar coordinates are used with ϕ as the angle and $\tan\theta$ as the radius, then the above equation is a straight line making intercepts on the [100] and [010] axes of $2h_{[001]}$. The directions of H for which hole orbits are just possible is a square of diagonal $4h_{[001]}$ in this gnomonic projection in which [001] is used as a pole. In Fig. 12 we show half of two such squares with the experimental points obtained for copper and silver.

The values of $2h_{[001]}$ found for copper and silver are $2h_{[001]}=0.21$ and $2h_{[001]}=0.19$, respectively. There is no obvious reason why the maxima for the various current directions should all lie on the same straight line, although the fit for the copper data appears very close. It may be that the more complicated open orbits occurring for arbitrary current directions are just combinations of the simpler orbits like [310] worked out above.

When H sweeps through the $[1\bar{1}0]$ pole, the closed hole orbits occur at an angle θ given by

$$\tan\theta \sin\phi = 2h_{[1\bar{1}0]}/\sqrt{3},$$

where $h_{[1\bar{1}0]}$ is the neck height in the $[1\bar{1}0]$ direction and ϕ is the angle between the current direction and the $[11\bar{1}]$ direction.

In a gnomonic projection with the pole in the direction $[1\bar{1}0]$ this is a straight line with intercepts of

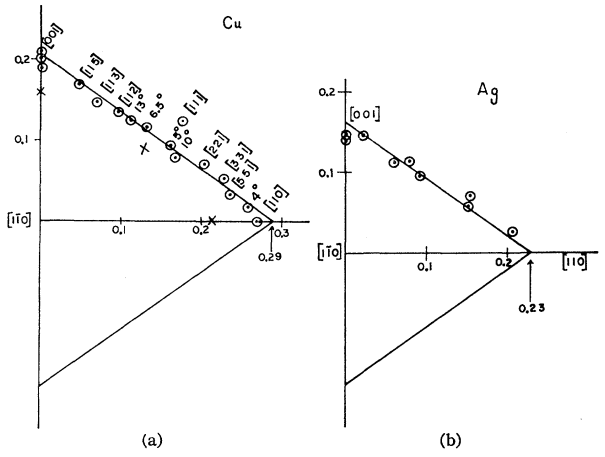

FIG. 13. Gnomonic projection of data obtained for the $[1\bar{1}0]$ pole. The half rhombs are drawn using the equation $\tan\theta \sin\phi = 2h_{[1\bar{1}0]}/\sqrt{3}$. ϕ and θ are again defined as in Fig. 12. (a) Data from copper. (b) Data from silver.

$2h_{[1\bar{1}0]}$ and $\sqrt{2}h_{[1\bar{1}0]}$ on the [110] and [001] directions, respectively. The region for existence of hole orbits is a rhomb and the appropriate rhombs for copper and silver are shown in Fig. 13. A fit with the experimental data gives $2h_{[1\bar{1}0]}=0.29$ for copper and $2h_{[1\bar{1}0]}=0.23$ for silver. It should be noted that there is twice the amount of information at this pole since for example [331] and [113] are independent current axes.

In the case of copper three experimental points are shown in Fig. 13(a) for the [001] current axis. Two of these points were obtained from the same crystal the smallest and largest values of θ being measured from two different ⟨110⟩ poles while the middle value was obtained from a different crystal. This variation in angle is probably due to the extreme sensitivity of the rotation diagram to orientation when the current is along a low-index direction. This was first pointed out by Klauder and Kunzler[4] for the [001] current axis. The "rabbit ears" which occur experimentally for the [001] axis have not been accounted for theoretically. The largest values of θ are obtained from poles for which the "rabbit ears" are smallest.

TABLE I. Comparison of experiment and theory for the magnetoresistance peaks near the [001] pole for four different current axes. The value of $A\xi/(\alpha m)^2$ is equal to the calculated magnetoresistance at the peak and should be compared to the experimental value of $\rho(H)/\rho(0)$.

Current axis	Exp. σ esu	Theo·ξ	Exp. $\rho(H)/\rho(0)$	$A\xi/(\alpha m)^2$
[310]	2.56×10^{21}	1.06	90	130
[210]	1.23×10^{21}	0.88	50	26
[110]	2.15×10^{21}	1.54	85	140
[100]	2.39×10^{21}	1.57	104	170

The large value of θ found for the [111] current directions can be accounted for from the calculation of the magnetoresistance for this current axis. The result is similar to Fig. 10 calculated for the [001] pole with J parallel to [110] and shows the resistance continuing to rise beyond the point where closed hole orbits first occur. This is indicated by the change of slope in Fig. 10.

The magnetoresistance curves calculated theoretically for field directions near the [001] pole were compared with the experimental measurements. In particular, a relaxation time was calculated from the residual resistance measurement for the [310] sample of copper. This was found to be $\tau=m\sigma/ne^2=1.2\times10^{-10}$ sec using the measured value of σ. The conductivity of the [310] sample at helium temperature was measured as 2.56×10^{21} esu which is consistent with a room temperature value listed in tables of 5.7×10^{17} esu for copper and gives a ratio of 4500 for this sample. Using the above value of the relaxation time, the calculated magnetoresistance at the peaks near [001] should be 130 times the zero-field resistance,

$$(A\xi/(\alpha m)^2=130).$$

The experimentally measured value of the ratio $\rho(H)/\rho(0)$ for the peak was 90. These results along with those from the other three axes for which the open orbits have been analyzed and the function ξ explicitly calculated are listed in Table I. We have listed the experimental value of the conductivity at helium temperature, the experimental value of the ratio $\rho(H)/\rho(0)$, the calculated value of ξ, and the calculated value of $A\xi/(\alpha m)^2$ at the peaks.

In three cases the value of $(A\xi/(\alpha m)^2)$ is higher than the experimental value of $\rho(H)/\rho(0)$ while for the [210] current axis $(A\xi/(\alpha m)^2)$ is lower than the experimental value $\rho(H)/\rho(0)$ by a factor of 2. The low experimental

[4] J. R. Klauder and J. E. Kunzler, in *The Fermi Surface*, edited by W. A. Harrison and M. B. Webb (John Wiley & Sons, Inc., New York, 1960), p. 125.

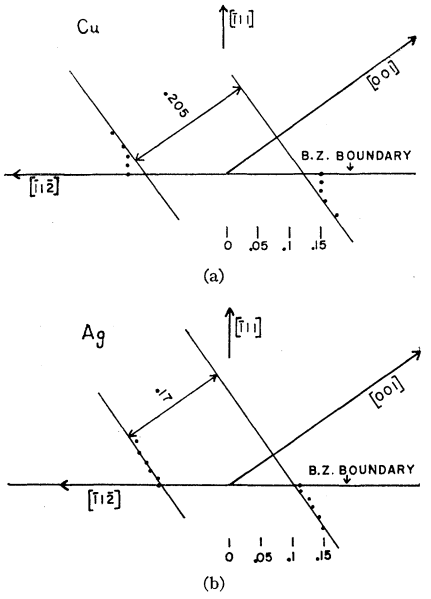

FIG. 14. Experimental points obtained by Bohm and Easterling (Ref. 2) for copper and silver using ultrasonic attenuation. (a) Drawing indicates projected neck thickness for copper in the [001] dirctioens; (b) drawing indicates projected neck thickness for silver in the [001] direction.

value of $\rho(H)/\rho(0)$ for the [210] axis relative to the others is due to the lower value of the conductivity and the fact that ξ has a smaller value for this current axis. The low value of ξ is due to the fact that the open orbits for the [210] current axis have longer periods (12 quarter-circles) than those found for the other current axes which were analyzed. This can be seen by comparing the orbits in Fig. 3 with the other orbits pictured in Figs. 1 to 5.

These results depend on the measurement of the zero-field potential drop across the sample, and this was measured with an accuracy of $\pm 1\times 10^{-8}$ V which corresponds to one division on the fine dial of the potentiometer. If the potential drop were in error by a factor $f\times$(potential drop), then the experimental value of $\rho(H)/\rho(0)$ would be multiplied by $1/f$ and the theoretical value by $1/f^2$. For example, the potential drop in zero field for the [310] axis was 0.025 ± 0.01 μV, and the maximum values of the factors $1/f$ and $1/f^2$ could therefore change the numbers in Table I on the order of 50%. Within this uncertainty the experimental and theoretical values are in fair agreement.

The theoretical results have been calculated using the assumption of an isotropic relaxation time. As discussed by Ziman,[5] this is probably not true and one might expect a considerable variation between, say, the belly and the neck of the Fermi surface. Information on this anisotropy in the relaxation time might be obtained by analyzing data obtained from samples with the same current axis containing different impurities. More accurate experimental measurements and more detailed analysis will be necessary, however, before any definite information can be obtained.

Slow rotation diagrams were run for a number of samples in order to pick up changes in slope in the resistance peaks such as predicted for ⟨310⟩ in copper (Fig. 7). A well-defined change was not observed in this sample, although a number of other samples did show a definite change in slope such as the experimental curve for silver shown in Fig. 11.

COMPARISON OF MAGNETORESISTANCE WITH MAGNETOACOUSTIC ATTENUATION

Bohm and Easterling[2] have made very complete measurements of the Fermi surface in all three noble metals using magnetoacoustic attenuation. In Fig. 14 we reproduce their results (in units of $b/2$) for the neck shape in the (110) plane for copper and silver. Two tangents have been drawn to the necks which are traces of (001) planes, i.e., they have the equations $z=\pm h$ and define the neck height in the [001] direction. As we have seen, the magnetoresistance measurements for H near the [001] pole give $2h_{[001]}=0.21$ for Cu and 0.19 for Ag which are in good agreement with 0.205 and 0.17, respectively, calculated using the data of Bohm and Easterling.

From Bohm and Easterling's data on Cu, it is clear that the open-orbit regions about the [001] pole will be limited by the curvature of the Fermi surface rather than by the neck diameter in the ($\bar{1}11$) plane. The importance of this curvature can be seen by calculating the neck thickness in the [$\bar{1}1\bar{2}$] direction assuming the open orbits to be limited only by the neck in the ($\bar{1}11$) plane. This gives 0.26 as calculated in a previous paper[6] which is considerably less than the value of 0.30 obtained by Bohm and Easterling. In the case of silver, the curvature does not seem to be as important in limiting the open orbit regions.

The magnetoresistance measurements with H near the [$1\bar{1}0$] pole give the thickness of the necks in the [$1\bar{1}0$] direction as 0.29 for Cu and 0.23 for Ag. The acoustic attenuation measurements of Bohm and Easterling give 0.30 for Cu and, assuming a circular neck, 0.22 for Ag (this is their measurement in the [$\bar{1}1\bar{2}$] direction).

ACKNOWLEDGMENTS

The authors would like to thank Phillip Sommer, Fritz Linke, and George Bartsch for valuable assistance in shop work and construction of the apparatus.

[5] J. M. Ziman, Phys. Rev. **121**, 1320 (1961).

[6] A. J. Funes and R. V. Coleman, Phys. Rev. **131**, 2084 (1963).